

# Gluonic excitations in lattice QCD: A brief survey

Colin Morningstar

*Department of Physics, Carnegie Mellon University, Pittsburgh, PA, USA 15213-3890*

**Abstract.** Our current knowledge about glueballs and hybrid mesons from lattice QCD simulations is briefly reviewed.

## INTRODUCTION

Hadronic states bound together by an *excited* gluon field, such as glueballs, hybrid mesons, and hybrid baryons, are a potentially rich source of information concerning the confining properties of QCD. Interest in such states has been recently sparked by observations of resonances with exotic  $1^{-+}$  quantum numbers[1] at Brookhaven. In fact, the proposed Hall D at Jefferson Lab will be dedicated to the search for hybrid mesons and one of the goals of CLEO-c will be to identify glueballs and exotics. Although our understanding of these states remains deplorable, recent lattice simulations have shed some light on their nature. In this talk, I summarize our current knowledge about glueballs and heavy- and light-quark hybrid mesons from lattice QCD simulations.

## GLUEBALLS

The glueball spectrum in the absence of virtual quark-antiquark pairs is now well known[2] and is shown in Fig. 1. The use of spatially coarse, temporally fine lattices with improved actions and the application of variational techniques to moderately-large matrices of correlations functions were crucial in obtaining this spectrum. Continuum limit results for the lowest-lying scalar and tensor states are in good agreement with recent previous calculations[3, 4] when expressed in terms of the hadronic scale  $r_0$ , the square root of the string tension  $\sqrt{\sigma}$ , or in terms of each other as a ratio of masses. Disagreements in specifying the masses of these states in GeV arise solely from ambiguities in setting the value of  $r_0$  within the quenched approximation. The glueball spectrum can be qualitatively understood in terms of the interpolating operators of minimal dimension which can create glueball states[5] and can be reasonably well explained[6] in terms of a simple constituent gluon (bag) model which approximates the gluon field using spherical cavity Hartree modes with residual perturbative interactions[7, 8]. The challenge now is to deduce precisely what the spectrum in Fig. 1 is telling us about the long-wavelength properties of QCD. This spectrum provides an important testing ground for

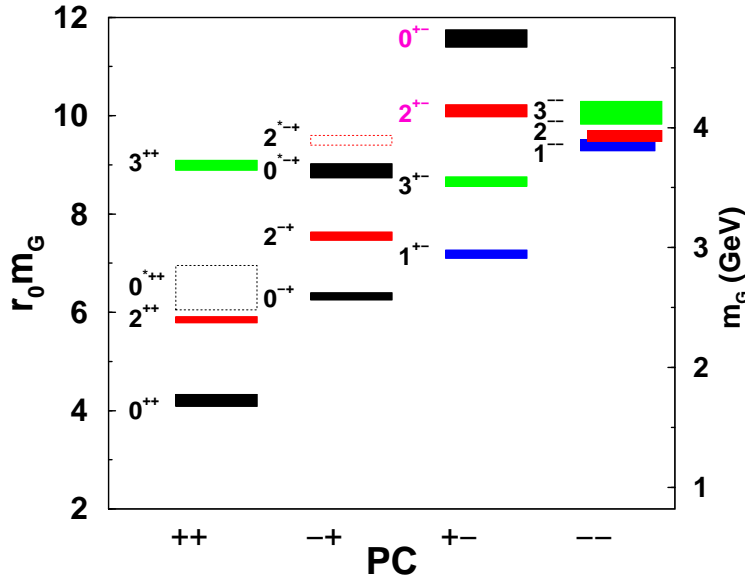


**FIGURE 1.** The mass spectrum of glueballs in the pure SU(3) gauge theory from Ref. [2]. The masses are given in terms of the hadronic scale  $r_0$  along the left vertical axis and in terms of GeV along the right vertical axis (assuming  $r_0^{-1} = 410(20)$  MeV). The mass uncertainties indicated by the vertical extents of the boxes do *not* include the uncertainty in setting  $r_0$ . The locations of states whose interpretation requires further study are indicated by the dashed hollow boxes.

models of confined gluons, such as center and Abelian dominance, instantons, soliton knots, instantaneous Coulomb-gauge mechanisms, and so on.

Recently, the two lowest-lying scalar glueballs and the tensor glueball have been studied[9] in  $SU(N)$  for  $N = 2, 3, 4$ , and 5. Their masses have been shown to depend linearly on  $1/N^2$ , and these masses in the limit  $N \rightarrow \infty$  do not differ substantially from

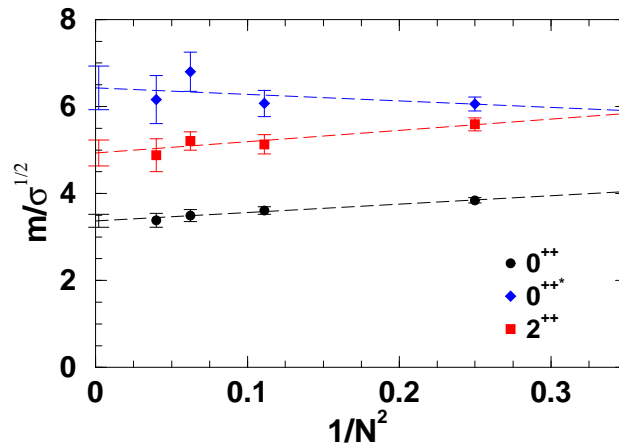


**FIGURE 2.** Continuum scalar, tensor, and excited scalar  $SU(N)$  glueball masses expressed in units of the string tension  $\sigma$  and plotted against  $1/N^2$ . Linear extrapolations to  $N = \infty$  are shown in each case (see Ref. [9]).

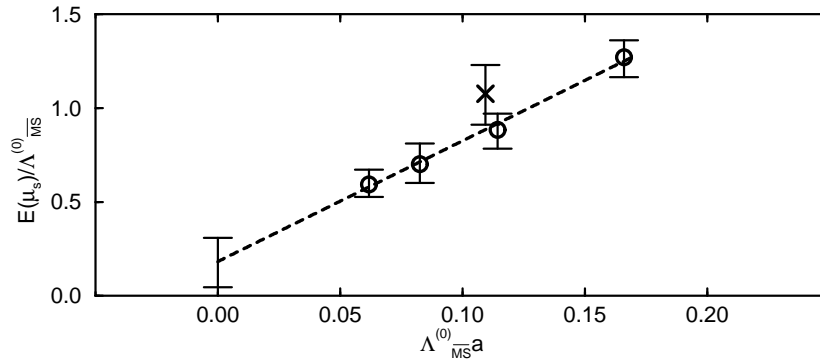


**FIGURE 3.** Lattice spacing dependence and continuum limit of the glueball-quarkonium mixing energy  $E(\mu_s)$  at the strange quark mass in the quenched approximation in terms of  $\Lambda_{\overline{MS}}^{(0)} = 234.9(6.2)$  MeV set using the (quenched) mass of the  $\rho$  meson. The continuum limit value of  $E(\mu_s)$  is 43(31) MeV. The circles indicate results using lattices with spatial extent approximately 1.6 fm; the  $\times$  indicates a result in a larger volume with spatial extent near 2.3 fm. (see Ref. [13]).

their values for small  $N$  (see Fig. 2).

Glueball wavefunctions and sizes have been studied in the past, but much of the early work contains uncontrolled systematic errors, most notably from discretization effects. The scalar glueball is particularly susceptible to such errors for the Wilson gauge action due to the presence of a critical end point of a line of phase transitions (not corresponding to any physical transition found in QCD) in the fundamental-adjoint coupling plane. As this critical point (which defines the continuum limit of a  $\phi^4$  scalar field theory) is neared, the coherence length in the scalar channel becomes large, which means that the mass gap in this channel becomes small; glueballs in other channels seem to be affected very little. Results in which the scalar glueball was found to be significantly smaller than the tensor were most likely due to contamination of the scalar glueball from the non-QCD critical point. In Ref. [10], an improved gauge action designed to avoid the spurious critical point found that the scalar and tensor glueballs were comparable in size and of typical hadronic dimensions. Operator overlaps obtained from the variational optimizations carried out in Ref. [2], which also used an improved gauge action, concur with such a conclusion.

Vacuum-to-glueball transition amplitudes for operators such as  $\langle G|\text{Tr}\mathbf{E}^2|0\rangle$  and  $\langle G|\text{Tr}\mathbf{B}^2|0\rangle$  in the  $0^{++}$  sector,  $\langle G|\text{Tr}\mathbf{E}\cdot\mathbf{B}|0\rangle$  in the  $0^{-+}$  sector, and  $\langle G|\text{Tr}\mathbf{E}_i\mathbf{E}_j|0\rangle$  in the  $2^{++}$  sector, have also been studied in the past[11]. Efforts to revisit these calculations using improved actions and operators with reduced discretization errors is ongoing.

A valiant effort to study the decay of the scalar glueball into two pseudoscalar mesons was made in Ref. [12]. A slight mass dependence of the coupling was found, and a total width of 108(29) MeV for decays to two pseudoscalars was obtained in the quenched approximation. However, these results were obtained with the Wilson gauge action at  $\beta = 5.7$ , an unfortunate choice since pollution of the scalar glueball from the non-QCD critical point is significant (for example, the mass differs from its continuum limit value by at least 20% and the mixing energy of the glueball with quarkonium differs dramatically from its continuum limit value as discussed below). These large systematic

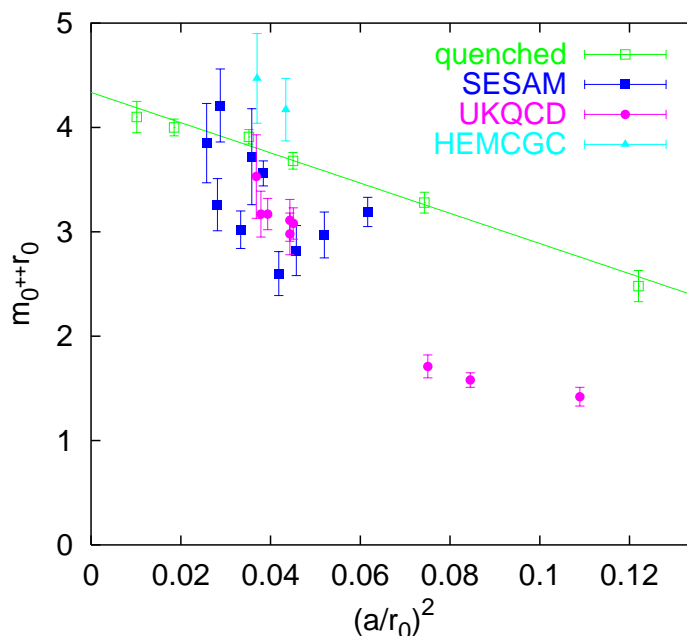


**FIGURE 4.** The scalar glueball mass with two flavors of virtual quark-antiquark pairs included against the lattice spacing  $a$  in terms of the hadronic scale  $r_0$ , courtesy of Ref. [18]. Results are shown for three different discretizations of the Dirac action: staggered (HEMCGC, from Ref. [14]), Wilson (SESAM from Ref. [15]), and clover (UKQCD from Refs. [16, 17]). The quarks are all heavier than a third of the strange quark mass. Quenched results are shown for comparison.

uncertainties and the use of the quenched approximation should be kept in mind when considering the value of the width given above.

Mixing of the scalar glueball with quarkonium has been studied in the quenched approximation in Ref. [13]. Several lattice spacings were used to facilitate control of discretization errors. Good control of systematic errors was demonstrated, although extrapolations in the quark mass to  $\mu_n$  (the  $u$  and  $d$  quark mass scale) might benefit from the use of chiral perturbation theory. The results for the mixing energy are shown in Fig. 3. Note that the continuum limit is essentially *consistent with zero mixing*. Again, remember that the inclusion of quark loops is incomplete when assessing this conclusion. The large variation of this mixing energy with the lattice spacing is most likely due to the use of the simple Wilson gauge action. The rightmost point corresponds to  $\beta = 5.7$  which illustrates the very large lattice artifacts at this spacing. This mixing calculation could benefit enormously from the use of an improved action and anisotropic lattices.

Incorporation of virtual quark-antiquark pairs in calculating the glueball/quarkonium spectrum is a daunting task. The fermion determinant must be included in the Monte Carlo updating, dramatically increasing the computational costs. Mixings with two meson states require all-to-all propagators, further adding to the cost and the stochastic uncertainties. Instabilities of the higher lying states must be properly taken into account (such as with finite volume techniques). Extrapolations to realistically light quark masses must be done carefully, taking decay thresholds into account and possibly requiring sim-

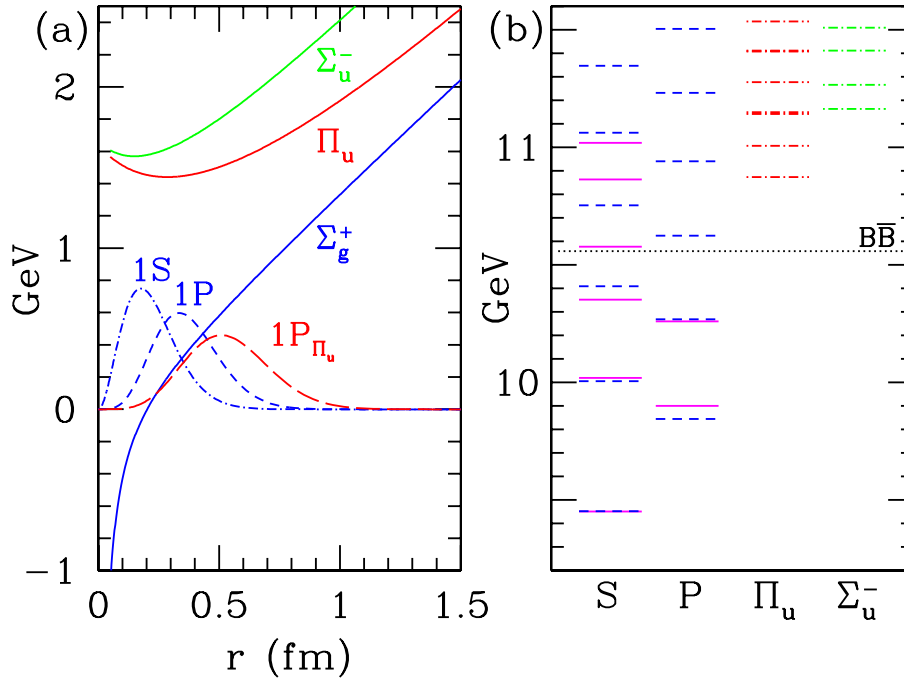


**FIGURE 5.** (a) Static potentials and radial probability densities against quark-antiquark separation  $r$  for  $r_0^{-1} = 450$  MeV. (b) Spin-averaged  $\bar{b}b$  spectrum in the LBO approximation (light quarks neglected). Solid lines indicate experimental measurements. Short dashed lines indicate the  $S$  and  $P$  state masses obtained using the  $\Sigma_g^+$  potential with  $M_b = 4.58$  GeV. Dashed-dotted lines indicate the hybrid quarkonium states obtained from the  $\Pi_u$  ( $L = 1, 2, 3$ ) and  $\Sigma_u^-$  ( $L = 0, 1, 2$ ) potentials. These results are from Ref. [22].

ulations to be carried out at quark masses lighter than currently feasible. Nevertheless, a few groups[14, 15, 16, 17] have begun glueball/meson simulations with two flavors of sea quarks, and the results for the scalar glueball mass are shown in Fig. 4. The status of such calculations has recently been reviewed in Ref. [18]. The quarks are still heavier than  $m_s/3$ , where  $m_s$  is the mass of the strange quark. The glueball mass tends to decrease as the light quark mass is reduced, but it increases as the lattice spacing is reduced, making it completely unclear what the end result will be in the continuum limit for realistically light quark masses.

## HEAVY-QUARK HYBRID MESONS

One expects that a heavy-quark meson can be treated similar to a diatomic molecule: the slow valence heavy quarks correspond to the nuclei and the fast gluon and light sea quark fields correspond to the electrons[19]. First, the quark  $Q$  and antiquark  $\bar{Q}$  are treated as static color sources and the energy levels of the fast degrees of freedom are determined as a function of the  $Q\bar{Q}$  separation  $r$ , each such energy level defining an adiabatic surface or potential. The motion of the slow heavy quarks is then described in the leading Born-Oppenheimer (LBO) approximation by the Schrödinger equation using each of these potentials. Conventional quarkonia are based on the lowest-lying potential;

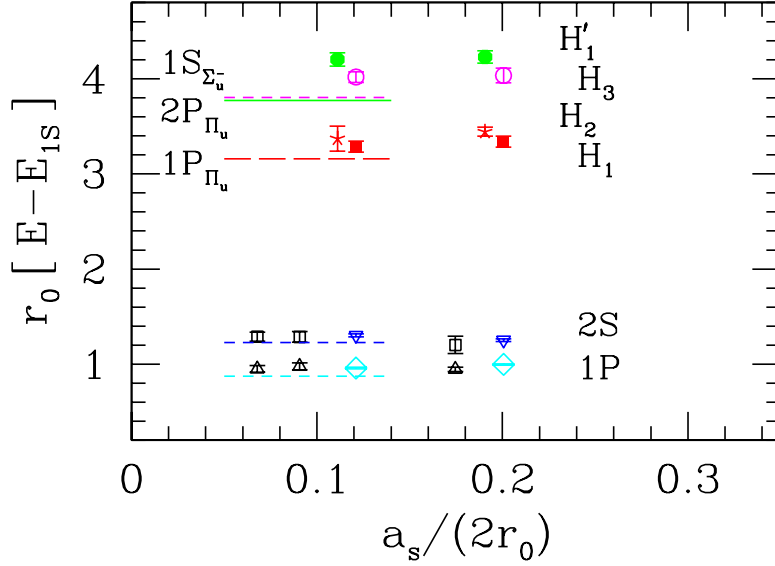


**FIGURE 6.** Simulation results from Ref. [22] for the heavy quarkonium level splittings (in terms of  $r_0$  and with respect to the  $1S$  state) against the lattice spacing  $a_s$ . Results from Ref. [25] using an NRQCD action with higher-order corrections are shown as open boxes and  $\triangle$ . The horizontal lines show the LBO predictions. Agreement of these splittings within 10% validates the Born-Oppenheimer approximation.

hybrid quarkonium states emerge from the excited potentials.

The spectrum of the fast gluon field in the presence of a static quark-antiquark pair has been determined in lattice studies[20, 21]. The three lowest-lying levels are shown in Fig. 5. Due to computational limitations, sea quark effects have been neglected in these calculations; their expected impact on the hybrid meson spectrum will be discussed below. The levels in Fig. 5 are labeled by the magnitude  $\Lambda$  of the projection of the total angular momentum  $\mathbf{J}_g$  of the gluon field onto the molecular axis, and by  $\eta = \pm 1$ , the symmetry under the charge conjugation combined with spatial inversion about the midpoint between the  $Q$  and  $\bar{Q}$ . States with  $\Lambda = 0, 1, 2, \dots$  are denoted by  $\Sigma, \Pi, \Delta, \dots$ , respectively. States which are even (odd) under the above-mentioned  $CP$  operation are denoted by the subscripts  $g$  ( $u$ ). An additional  $\pm$  superscript for the  $\Sigma$  states refers to even or odd symmetry under a reflection in a plane containing the molecular axis. The potentials are calculated in terms of the hadronic scale parameter  $r_0$ ; in Fig. 5,  $r_0^{-1} = 450$  MeV has been assumed.

The LBO spectrum[22] of conventional  $\bar{b}b$  and hybrid  $\bar{b}gb$  states are shown in Fig. 5. Below the  $\bar{B}B$  threshold, the LBO results are in very good agreement with the spin-averaged experimental measurements of bottomonium states. Above the threshold, agreement with experiment is lost, suggesting significant corrections either from mixing and other higher-order effects or (more likely) from light sea quark effects. Note from the radial probability densities shown in Fig. 5 that the size of the hybrid state is large in comparison with the conventional  $1S$  and  $1P$  states.

The validity of such a simple physical picture relies on the smallness of higher-order spin, relativistic, and retardation effects and mixings between states based on different adiabatic surfaces. The importance of retardation and leading-order mixings between

states based on different adiabatic potentials can be tested by comparing the LBO level splittings with those determined from meson simulations using a leading-order non-relativistic (NRQCD) heavy-quark action. Such a test was carried out in Ref. [22]. The NRQCD action included only a covariant temporal derivative and the leading kinetic energy operator (with two other operators to remove lattice spacing errors). The only difference between the leading Born-Oppenheimer Hamiltonian and the lowest-order NRQCD Hamiltonian was the  $\mathbf{p}\cdot\mathbf{A}$  coupling between the quark color charge in motion and the gluon field. The level splittings (in terms of  $r_0$  and with respect to the  $1S$  state) of the conventional  $2S$  and  $1P$  states and four hybrid states were compared (see Fig. 6) and found to agree within 10%, strongly supporting the validity of the leading Born-Oppenheimer picture.

The question of whether or not quark spin interactions spoil the validity of the Born-Oppenheimer picture for heavy-quark hybrids has been addressed in Ref. [23]. Simulations of several hybrid mesons using an NRQCD action including the spin interaction  $c_B\boldsymbol{\sigma}\cdot\mathbf{B}/2M_b$  and neglecting light sea quark effects were carried out; the introduction of the heavy-quark spin was shown to lead to significant level shifts (of order 100 MeV or so) but the authors of Ref. [23] argue that these splittings do *not* signal a breakdown of the Born-Oppenheimer picture. First, they claim that no significant mixing of their non-exotic  $0^{-+}$ ,  $1^{--}$ , and  $2^{-+}$  hybrid meson operators with conventional states was observed; unfortunately, this claim is not convincing since a correlation matrix analysis was not used. Secondly, the authors argue that calculations using the bag model support their suggestion. These facts are not conclusive evidence that heavy-quark spin effects do not spoil the Born-Oppenheimer picture, but they are highly suggestive. Further evidence to support the Born-Oppenheimer picture has recently emerged in Ref. [24]. The NRQCD simulations carried out in this work examined the mixing of the  $\Upsilon$  with a hybrid and found a very small probability admixture of hybrid in the  $\Upsilon$  given by  $0.0035(1)c_B^2$  where  $c_B^2 \sim 1.5 - 3$  is expected.

The dense spectrum of hybrid states shown in Fig. 5 neglects the effects of light sea quark-antiquark pairs. In order to include these effects in the LBO, the adiabatic potentials must be determined fully incorporating the light quark loops. Such computations using lattice simulations are very challenging, but good progress is being made. For separations below 1 fm, the  $\Sigma_g^+$  and  $\Pi_u$  potentials change very little[15] upon inclusion of the sea quarks (see Fig. 7), suggesting that a few of the lowest-lying hybrid states may exist as well-defined resonances. However, for  $Q\bar{Q}$  separations greater than 1 fm, the adiabatic surfaces change dramatically, as shown in Fig. 8 from Ref. [26]. Instead of increasing indefinitely, the static potential abruptly levels off at a separation of 1 fm when the static quark-antiquark pair, joined by flux tube, undergoes fission into two separate  $\bar{Q}q$  color singlets, where  $q$  is a light quark. Clearly, such potentials cannot support the plethora of conventional and hybrid states shown in Fig. 5; the formation of bound states and resonances substantially extending over 1 fm seems unlikely. Whether or not the light sea quark-antiquark pairs spoil the Born-Oppenheimer picture is currently unknown. Future unquenched simulations should help to answer this question, but it is not unreasonable to speculate that the simple physical picture provided by the Born-Oppenheimer expansion for both the low-lying conventional and hybrid heavy-quark mesons will survive the introduction of the light sea quark effects. Note that the discrep-

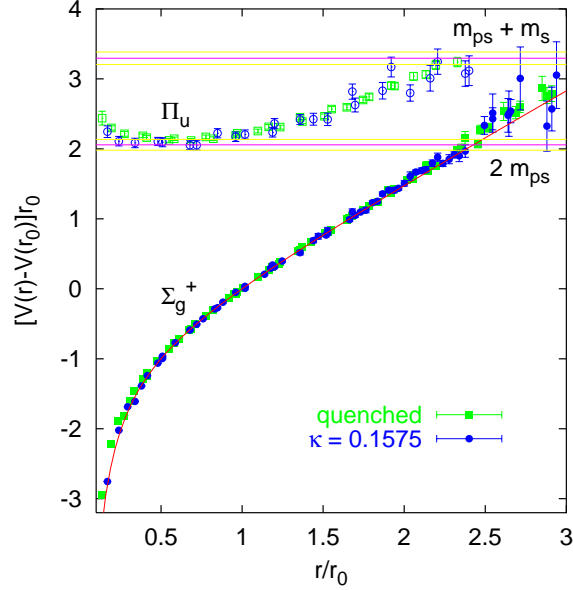


**FIGURE 7.** Ground  $\Sigma_g^+$  and first-excited  $\Pi_u$  static quark potentials without sea quarks (squares, quenched) and with two flavors of sea quarks, slightly lighter than the strange quark (circles,  $\kappa = 0.1575$ ). Results are given in terms of the scale  $r_0 \approx 0.5$  fm, and the lattice spacing is  $a \approx 0.08$  fm. Note that  $m_S$  and  $m_{PS}$  are the masses of a scalar and pseudoscalar meson, respectively, consisting of a light quark and a static antiquark. These results are from Ref. [15].

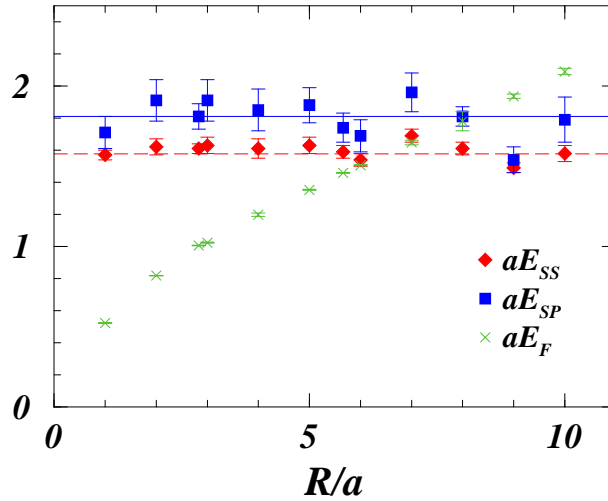


**FIGURE 8.** Evidence for “string breaking” at quark-antiquark separations  $R \approx 1$  fm.  $E_{SS}$  is the energy of two  $S$ -wave static-light mesons (the light quark bound in an  $S$ -wave to the fixed static antiquark),  $E_{SP}$  is the energy of an  $S$ -wave and a  $P$ -wave static-light meson, and  $E_F$  is the energy of a static quark-antiquark pair connected by a gluonic flux tube. The distance of separation  $R$  refers to the distance between the static quark-antiquark pair. All quantities are measured in terms of the lattice spacing  $a \approx 0.16$  fm. Two flavors of light sea quarks are present with masses such that  $m_\pi/m_\rho \approx 0.36$ . The dashed and solid lines give the asymptotic values  $2am_S$  and  $a(m_P + m_S)$ , where  $m_S$  and  $m_P$  are the masses of individual  $S$ -wave and  $P$ -wave static-light mesons, respectively. Mixing between the flux tube and meson-meson channels was found to be very weak. Results are from Ref. [26].



**TABLE 1.** Recent results for the light quark and charmonium  $1^{-+}$  hybrid meson masses. Method abbreviations: W = Wilson fermion action; SW = improved clover fermion action; NR = nonrelativistic heavy quark action.  $N_f$  is the number of dynamical light quark flavors used.

Light quark $1^{-+}$				Charmonium $1^{-+} - 1S$		
Ref. & Method	$N_f$	$M$ (GeV)		Ref. & Method	$\Delta M$ (GeV)	
UKQCD 97[27]	SW	0	1.87(20)	MILC 97[28]	W	1.34(8)(20)
MILC 97[28]	W	0	1.97(9)(30)	MILC 99[29]	SW	1.22(15)
MILC 99[29]	SW	0	2.11(10)	CP-PACS 99[31]	NR	1.323(13)
LaSch 99[30]	W	2	1.9(2)	JKM 99[22]	LBO	1.19

ancies of the spin-averaged LBO predictions with experiment above the  $B\bar{B}$  threshold seen in Fig. 5 most likely arise from the neglect of light sea quark-antiquark pairs.

## LIGHT-QUARK HYBRID MESONS

A summary of recent light-quark and charmonium  $1^{-+}$  hybrid mass calculations is presented in Table 1. With the exception of Ref. [30], all results neglect light sea quark loops. The introduction of two flavors of dynamical quarks in Ref. [30] yielded little change to the hybrid mass, but this finding should not be considered definitive due to uncontrolled systematics (unphysically large quark masses, inadequate treatment of resonance properties in finite volume, *etc.*). All estimates of the light quark hybrid mass are near 2.0 GeV, well above the experimental candidates found in the range 1.4-1.6 GeV. Perhaps sea quark effects will resolve this discrepancy, or perhaps the observed states are *not* hybrids. Some authors have suggested that they may be four quark  $\bar{q}\bar{q}qq$  states. Clearly, there is still much to be learned about these exotic QCD resonances.

## CONCLUSION AND OUTLOOK

Our current understanding of hadronic states containing excited glue is poor, but recent lattice simulations have shed some light on their properties. The glueball spectrum in the pure gauge theory is now well known, and pioneering studies of the mixings of the scalar glueball with scalar quarkonia suggests that these mixings may actually be small. The validity of a Born-Oppenheimer treatment for heavy-quark mesons, both conventional and hybrid, has been verified at leading order in the absence of light sea quark effects, and quark spin interactions do not seem to spoil this. Progress in including the light sea quarks is also being made, and it seems likely that a handful of heavy-quark hybrid states might survive their inclusion. Of course, much more work is needed. The inner structure of glueballs and flux tubes will be probed. Future lattice simulations should provide insight into hybrid meson production and decay mechanisms and the spectrum and nature of hybrid baryons; virtually nothing is known about either of these topics. Glueballs, hybrid mesons, and hybrid baryons, remain a potentially rich source of information (and perhaps surprises) about the confining properties of QCD. This work

was supported by the U.S. National Science Foundation under award PHY-0099450.

## REFERENCES

1. D. Thompson *et al.*, Phys. Rev. Lett. **79**, 1630 (1997); G. Adams *et al.*, Phys. Rev. Lett. **81**, 5760 (1998); A. Abele *et al.*, Phys. Lett. **B423**, 175 (1998).
2. C. Morningstar and M. Peardon, Phys. Rev. D **60**, 034509 (1999).
3. G. Bali *et al.* (UKQCD Collaboration), Phys. Lett. B **309**, 378 (1993).
4. A. Vaccarino and D. Weingarten, Phys. Rev. D **60**, 114501 (1999).
5. R.L. Jaffe, K. Johnson, and Z. Ryzak, Ann. Phys. **168**, 344 (1986).
6. J. Kuti, Nucl. Phys. (Proc. Suppl.) **73**, 72 (1999).
7. T. Barnes, F. Close, and S. Monaghan, Nucl. Phys. **B198**, 380 (1982).
8. C. Carlson, T. Hansson, and C. Peterson, Phys. Rev. D **27**, 1556 (1983).
9. B. Lucini and M. Teper, JHEP 06(2001)050.
10. R. Gupta, A. Patel, C. Baillie, G. Kilcup, and S. Sharpe, Phys. Rev. D **43**, 2301 (1991).
11. Y. Liang *et al.*, Phys. Lett. **B307**, 375 (1993); S.J. Dong *et al.*, Nucl. Phys. (Proc. Suppl.) **63**, 254 (1998).
12. J. Sexton, A. Vaccarino, and D. Weingarten, Phys. Rev. Lett. **75**, 4563 (1995).
13. W.J. Lee and D. Weingarten, Phys. Rev. D **61**, 014015 (2000).
14. K.M. Bitar *et al.*, Phys. Rev. D **44**, 2090 (1991).
15. G.S. Bali *et al.*, Phys. Rev. D **62**, 054503 (2000).
16. C. McNeile and C. Michael, Phys. Rev. D **63**, 114503 (2001).
17. A. Hart and M. Teper, hep-lat/0108022.
18. G. Bali, proceedings of Photon 2001, Ascona, Switzerland, Sep 2001 (hep-ph/0110254).
19. P. Hasenfratz, R. Horgan, J. Kuti, J. Richard, Phys. Lett. **B95**, 299 (1980).
20. K.J. Juge, J. Kuti, and C. Morningstar, Nucl. Phys. B(Proc. Suppl.) **63** 326, (1998); and hep-lat/9809098.
21. S. Perantonis and C. Michael, Nucl. Phys. **B347**, 854 (1990).
22. K.J. Juge, J. Kuti, and C. Morningstar, Phys. Rev. Lett. **82**, 4400 (1999).
23. I. Drummond, N. Goodman, R. Horgan, H. Shanahan, and L. Storti, Phys. Lett. **B478**, 151 (2000).
24. T. Burch, K. Orginos, and D. Toussaint, Phys. Rev. D **64**, 074505 (2001).
25. C. Davies *et al.*, Phys. Rev. **D58**, 054505 (1998).
26. C. Bernard *et al.*, Phys. Rev. D **64**, 074509 (2001).
27. P. Lacey *et al.*, Phys. Lett. **B401**, 308 (1997).
28. C. Bernard *et al.*, Phys. Rev. **D56**, 7039 (1997).
29. C. Bernard *et al.*, Nucl. Phys. B(Proc. Suppl.) **73**, 264 (1999).
30. P. Lacey and K. Schilling, Nucl. Phys. B(Proc. Suppl.) **73**, 261 (1999).
31. T. Manke *et al.*, Phys. Rev. Lett. **82**, 4396 (1999).